Resonance Raman Spectroscopy as a Probe of the Bis(μ-oxo)dicopper Core

Patrick L. Holland, Christopher J. Cramer,* Elizabeth C. Wilkinson, Samiran Mahapatra, Kenton R. Rodgers,† Shinobu Itoh,‡ Masayasu Taki,‡ Shunichi Fukuzumi,‡ Lawrence Que, Jr.,* and William B. Tolman*

Contribution from the Department of Chemistry, Center for Metals in Biocatalysis, and Supercomputer Institute, University of Minnesota, 207 Pleasant St. SE, Minneapolis, Minnesota 55455, the Department of Chemistry, North Dakota State University, P.O. Box 5516, Fargo, North Dakota 58105, and the Department of Applied Chemistry, Osaka University, 2-1 Yamada-oka, Suita, Osaka 565, Japan

Received June 14, 1999

Abstract: Resonance Raman spectra of dicopper complexes $[L_2Cu_2(\mu\text{-}O)_2]^{2+}$ contain a number of resonance-enhanced features between 500 and 900 cm^{-1}, with L = R_3TACN and various bidentate ligands (TACN = 1,4,7-triazacyclononane). Most importantly, there is a vibration near 600 cm^{-1} in all $[L_2Cu_2(\mu\text{-}O)_2]^{2+}$ compounds that is polarized, shifts by 19−27 cm^{-1} upon $^{18}O_2$ substitution, and gives a new peak with $^{16}O^{18}O$ substitution, identifying it as a totally symmetric A_g vibration of the bis(μ-oxo)dicopper(III) core. Changing the pendant groups on R_3TACN causes shifts in the frequency of the $Cu_2(\mu\text{-}O)_2$ vibration, but the direction of these shifts depends on the details of the organic fragment. A substantial shift to higher frequency is evident when bidentate ligands are used in place of TACN. Importantly, bidentate ligands with two different types of nitrogen donors show two independent core vibrations; these are assigned as "breathing" and "pairwise" modes through simple group theory considerations as well as by calculations using density functional theory. These calculations are extended to examine systematic trends with ligand variation as well as potential excited-state distortions of the core. Finally, the symmetry and energy of the $Cu_2(\mu\text{-}O)_2$ vibrations are compared with resonance Raman data for other biologically relevant high-valent $M_2(\mu\text{-}O)_2$ cores (M = Fe, Mn) to derive lessons for examining biological and model systems.

Introduction

The bis(μ-oxo)dimetal $[M_2(\mu\text{-}O)_2]^{n+}$ core has been proposed as a common motif for oxidation chemistry mediated by manganese, iron, and copper metalloenzymes.[1,2] For example, water oxidation during photosynthesis occurs at a tetramanganese cluster shown by spectroscopic studies to contain $[Mn_2(\mu\text{-}O)_2]^{n+}$ units.[3] X-ray absorption fine structure (EXAFS) and Mössbauer studies of the intermediate directly responsible for the oxidation of alkanes by soluble methane monooxygenase (compound Q) support an $[Fe^{IV}_2(\mu\text{-}O)_2]^{4+}$ formulation, possibly with additional bridging groups.[4] The catalytically essential tyrosyl radical (Y122•) in ribonucleotide reductase is generated from an intermediate, termed X, that has a core that is best described as $Fe^{III}Fe^{IV}$ [5] and appears by Mössbauer spectroscopy to be very similar to that generated by reducing Q by one electron.[6] These results suggest that X may have a similar $[Fe^{III}Fe^{IV}(\mu\text{-}O)_2]^{3+}$ core, although alternative structures for Q and X have been proposed.[7] Thus, studying complexes with $[M_2(\mu\text{-}O)_2]^{n+}$ cores may help us to understand the oxidations of water, methane, and tyrosine in nature. In addition to these biological centers, synthetic complexes containing the $[M_2(\mu\text{-}O)_2]^{n+}$ (M = Fe or Mn) cores have been characterized, leading to insights into their structural and physicochemical signatures.[1,8−10]

The characterization of compounds with $[Cu^{III}_2(\mu\text{-}O)_2]^{2+}$ cores,[11] derived from reaction of copper(I) complexes with dioxygen, has raised the possibility that such $[M_2(\mu\text{-}O)_2]^{n+}$

† North Dakota State University.

‡ Osaka University.

(1) (a) Que, L., Jr.; Dong, Y. *Acc. Chem. Res.* **1996**, *29*, 190−196. (b) Que, L., Jr. *J. Chem. Soc., Dalton Trans.* **1997**, 3933−3940.

(2) Tolman, W. B. *Acc. Chem. Res.* **1997**, *30*, 227−237.

(3) (a) Yachandra, V. K.; Sauer, K.; Klein, M. P. *Chem. Rev.* **1996**, *96*, 2927−2959. (b) Tommos, C.; Babcock, G. T. *Acc. Chem. Res.* **1998**, *31*, 18−25.

(4) Shu, L.; Nesheim, J. C.; Kauffmann, K.; Münck, E.; Lipscomb, J. D.; Que, L., Jr. *Science* **1997**, *275*, 515−518.

(5) Wallar, B. J.; Lipscomb, J. D. *Chem. Rev.* **1996**, *96*, 2625−2657.

(6) Valentine, A. M.; Tavares, P.; Pereira, A. S.; Davydov, R.; Krebs, C.; Hoffman, B. M.; Edmondson, D. R.; Huynh, B. H.; Lippard, S. J. *J. Am. Chem. Soc.* **1998**, *120*, 2190−2191.

(7) (a) Liu, K. E.; Johnson, C. C.; Newcomb, M.; Lippard, S. J. *J. Am. Chem. Soc.* **1993**, *115*, 939−947. (b) Sturgeon, B. E.; Burdi, D.; Chen, S.; Huynh, B.-H.; Edmondson, D. E.; Stubbe, J.; Hoffman, B. M. *J. Am. Chem. Soc.* **1996**, *118*, 7551−7557. (c) Siegbahn, P. E. M.; Crabtree, R. H. *J. Am. Chem. Soc.* **1997**, *119*, 3103−3133. (d) Riggs-Gelasco, P. J.; Shu, L.; Chen, S.; Burdi, D.; Huynh, B. H.; Que, L., Jr.; Stubbe, J. *J. Am. Chem. Soc.* **1998**, *120*, 849−860. (e) Burdi, D.; Willems, J.-P.; Riggs-Gelasco, P.; Antholine, W. E.; Stubbe, J.; Hoffman, B. M. *J. Am. Chem. Soc.* **1998**, *120*, 12910−12919.

(8) (a) Manchanda, R.; Brudvig, G. W.; Crabtree, R. H. *Coord. Chem. Rev.* **1995**, *144*, 1−38. (b) Pecoraro, V. C.; Baldwin, M. J.; Gelasco, A. *Chem. Rev.* **1994**, *94*, 807−826. (c) Wieghardt, K. *Angew. Chem., Int. Ed. Engl.* **1989**, *28*, 1153−1172.

(9) Dong, Y.; Fujii, H.; Hendrich, M. P.; Leising, R. A.; Pan, G.; Randall, C. R.; Wilkinson, E. C.; Zang, Y.; Que, L., Jr.; Fox, B. G.; Kauffmann, K.; Münck, E. *J. Am. Chem. Soc.* **1995**, *117*, 2778−2792.

(10) Hsu, H.-F.; Dong, Y.; Shu, L.; Young, V. G., Jr.; Que, L., Jr. *J. Am. Chem. Soc.* **1999**, *121*, 5230−5237.

(11) The formal oxidation state of copper in these bis(μ-oxo)dicopper complexes is +3, a description experimentally supported by X-ray absorption spectroscopy.[11a] The copper−oxygen bonding is highly covalent, however.[11b] (a) DuBois, J. L.; Mukherjee, P.; Collier, A. M.; Mayer, J. M.; Solomon, E. I.; Hedman, B.; Stack, T. D. P.; Hodgson, K. O. *J. Am. Chem. Soc.* **1997**, *119*, 8578−8579. (b) Cramer, C. J.; Smith, B. A.; Tolman, W. B. *J. Am. Chem. Soc.* **1996**, *118*, 11283−11287.

10.1021/ja992003l CCC: $19.00
Published on Web 01/22/2000

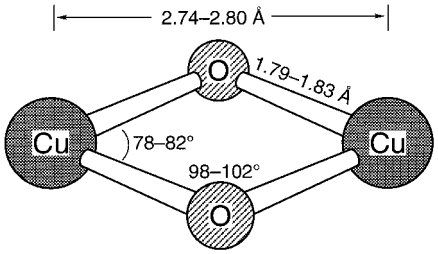

Figure 1. Perspective view of the $[Cu_2(\mu\text{-}O)_2]^{2+}$ core derived from the X-ray crystal structure of $[(Bn_3TACN)_2Cu_2(\mu\text{-}O)_2](SbF_6)_2$, showing the range of metrical parameters from the three X-ray structural studies of these cores.[13−15]

intermediates are also involved in oxidation chemistry mediated by copper-containing enzymes[12] and abiological catalysts. X-ray crystallographic and EXAFS studies of complexes that contain the $[Cu_2(\mu\text{-}O)_2]^{2+}$ core have shown that it is a planar, symmetric Cu_2O_2 rhomb with short copper−oxygen and copper−copper distances of 1.8 and 2.8 Å, respectively (Figure 1).[2,13−15] Recent research efforts with bis(μ-oxo)dicopper complexes capped by 1,4,7-trisubstituted 1,4,7-triazacyclononanes (R_3TACN, Chart 1) have focused on the interconversion of the core with its (μ-η^2:η^2-peroxo)dicopper isomer,[11b,13,16,17] its theoretical characterization by ab initio calculations,[11b,18] the mechanism of its oxidative reactions,[19] and the effects of turning the R_3TACN into a binucleating ligand.[14,20] Complementary studies by Stack and co-workers have shown that bidentate amine donor ligands also can support the $[Cu_2(\mu\text{-}O)_2]^{2+}$ core,[15] and Karlin and co-workers have provided evidence for this core in complexes with tridentate pyridine-containing ligands.[21] We also have found that bis(μ-oxo)dicopper complexes with bidentate, mixed pyridyl/amine donor ligands are capable of hydroxylating both pendant aromatic[22] and aliphatic[23] groups.

Chart 1

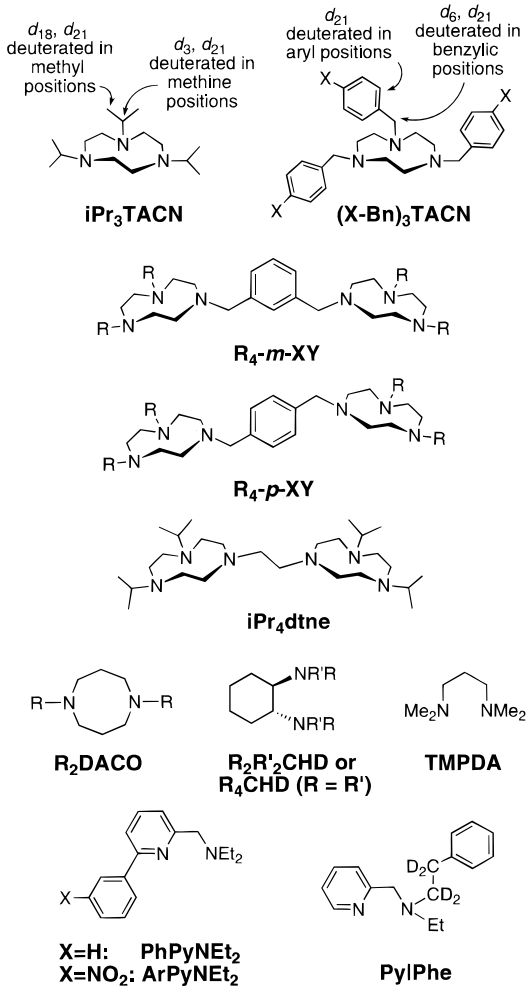

The possibility that nature uses $[M_2(\mu\text{-}O)_2]^{n+}$ groups as reactive intermediates with three different metals has provided the impetus to undertake detailed spectroscopic studies of synthetic complexes containing these cores. Common spectral features include electronic absorptions in the visible region that are assigned as ligand-to-metal ($O^{2-} \rightarrow M^{x+}$) charge-transfer transitions on the basis of their intensity and the high formal oxidation state of the metals. Resonance Raman (RR) spectra obtained by excitation into these charge-transfer bands in model complexes that contain $[Mn_2(\mu\text{-}O)_2]^{n+}$ [24−26] and $[Fe_2(\mu\text{-}O)_2]^{3+}$ cores[9,27] have an intense feature in the 650−710 cm^{-1} region. In initial reports of $[Cu_2(\mu\text{-}O)_2]^{2+}$ complexes, similar bands were noted at about 600 cm^{-1},[13] and this recurrent feature was assigned as a characteristic vibration of the bis(μ-oxo)dicopper core. However, this vibration was not assigned to a specific normal mode of the core.

In this study, we analyze RR data for a wide range of bis(μ-oxo)dicopper compounds supported by ligands of varying structure. Although many of these are capped by tridentate TACN ligands, bidentate amine ligands as well as bidentate and tridentate imine/amine ligands have been used comparatively to understand the vibrational features of this important type of

(12) Solomon, E. I.; Sundaram, U. M.; Machonkin, T. E. *Chem. Rev.* **1996**, *96*, 2563−2605.
(13) Mahapatra, S.; Halfen, J. A.; Wilkinson, E. C.; Pan, G.; Wang, X.; Young, V. G., Jr.; Cramer, C. J.; Que, L., Jr.; Tolman, W. B. *J. Am. Chem. Soc.* **1996**, *118*, 11555−11574.
(14) Mahapatra, S.; Young, V. G., Jr.; Kaderli, S.; Zuberbühler, A. D.; Tolman, W. B. *Angew. Chem., Int. Ed. Engl.* **1997**, *36*, 130−133.
(15) Mahadevan, V.; Hou, Z.; Cole, A. P.; Root, D. E.; Lal, T. K.; Solomon, E. I.; Stack, T. D. P. *J. Am. Chem. Soc.* **1997**, *119*, 11996−11997.
(16) Halfen, J. A.; Mahapatra, S.; Wilkinson, E. C.; Kaderli, S.; Young, V. G., Jr.; Que, L., Jr.; Zuberbühler, A. D.; Tolman, W. B. *Science* **1996**, *271*, 1397−1400.
(17) (a) Cahoy, J.; Holland, P. L.; Tolman, W. B. *Inorg. Chem.* **1999**, *38*, 2161−2168. (b) Holland, P. L.; Tolman, W. B. *Coord. Chem. Rev.* **1999**, *190*−*192*, 855−869.
(18) (a) Bérces, A. *Inorg. Chem.* **1997**, *36*, 4831−4837. (b) Liu, X.-Y.; Palacios, A. A.; Novoa, J. J.; Alvarez, S. *Inorg. Chem.* **1998**, *37*, 1202−1212. (c) Yoshizawa, K.; Ohta, T.; Yamabe, T. *Bull. Chem. Soc. Jpn.* **1997**, *70*, 1911−1917. (d) Eisenstein, O.; Getlicherman, H.; Giessner-Prettre, C.; Maddaluno, J. *Inorg. Chem.* **1997**, *36*, 3455−3460. (e) Estiú, G. L.; Zerner, M. C. *J. Am. Chem. Soc.* **1999**, *121*, 1893−1901. (f) Flock, M.; Pierloot, K. *J. Phys. Chem. A* **1999**, *103*, 95−102.
(19) (a) Mahapatra, S.; Halfen, J. A.; Tolman, W. B. *J. Am. Chem. Soc.* **1996**, *118*, 11575−11586. (b) Berreau, L. M.; Mahapatra, S.; Halfen, J. A.; Houser, R. P.; Young, V. G., Jr.; Tolman, W. B. *Angew. Chem., Int. Ed.* **1999**, *38*, 207−210.
(20) Mahapatra, S.; Kaderli, S.; Llobet, A.; Neuhold, Y.-M.; Palanché, T.; Halfen, J. A.; Young, V. G., Jr.; Kaden, T. A.; Que, L., Jr.; Zuberbühler, A. D.; Tolman, W. B. *Inorg. Chem.* **1997**, *36*, 6343−6356.
(21) (a) Obias, H. V.; Lin, Y.; Murthy, N. N.; Pidcock, E.; Solomon, E. I.; Ralle, M.; Blackburn, N. J.; Neuhold, Y.-M.; Zuberbühler, A. D.; Karlin, K. D. *J. Am. Chem. Soc.* **1998**, *120*, 12960−12961. (b) Pidcock, E.; Obias, H. V.; Abe, M.; Liang, H.-C.; Karlin, K. D.; Solomon, E. I. *J. Am. Chem. Soc.* **1999**, *121*, 1299−1308. (c) Pidcock, E.; DeBeer, S.; Obias, H. V.; Hedman, B.; Hodgson, K. O.; Karlin, K. D.; Solomon, E. I. *J. Am. Chem. Soc.* **1999**, *121*, 1870−1878.
(22) Holland, P. L.; Rodgers, K. R., Tolman, W. B. *Angew. Chem., Int. Ed.* **1999**, *38*, 1139−1142.
(23) Itoh, S.; Taki, M.; Nakao, H.; Holland, P. L.; Tolman, W. B.; Que, L. Jr.; Fukuzumi, S. *Angew. Chem., Int. Ed.* **2000**, *39*, in press.
(24) Czernuszewicz, R. S.; Dave, B.; Rankin, J. G. In *Spectroscopy of Biological Molecules*; Hester, R. E., Girling, R. B., Eds.; Royal Society of Chemistry: Cambridge, 1991; pp 285−288.
(25) Dave, B. C.; Czernuszewicz, R. S. *Inorg. Chim. Acta* **1994**, *227*, 33−41.
(26) Dave, B. C.; Czernuszewicz, R. S. *Inorg. Chim. Acta* **1998**, *281*, 25−35.

copper−oxygen complex. The characteristic 600 cm^{-1} vibration is shown to correspond to a "breathing" vibration of the entire $[Cu_2(\mu\text{-}O)_2]^{2+}$ core, and the effects of oxygen isotope substitution and of ligand deuteration, substitution, and geometry on this vibration are elucidated by using experimental and theoretical methods. Importantly, spectra of complexes with ligands containing two different nitrogen donors show a second Raman-active vibration of the $[Cu_2(\mu\text{-}O)_2]^{2+}$ core, and ab initio calculations are used (a) to support an assignment of this vibration and (b) to address the effects of ligand asymmetry. Finally, comparison of the copper system to iron and manganese analogues lets one draw general conclusions about the vibrational properties of $[M_2(\mu\text{-}O)_2]^{n+}$ cores.

Results

Resonance Raman Spectroscopy of $[L_2Cu_2(\mu\text{-}O)_2]^{2+}$ Complexes With Triazacyclononane Ligands. The electronic spectra of these bis(μ-oxo)dicopper complexes contain two characteristic features at 300−330 and 400−450 nm attributable to oxo-to-metal charge-transfer transitions.[13,15] These bands are of high intensity ($>10^4$ M^{-1} cm^{-1}), consistent with a large degree of covalency in the Cu−O bonds of the $[Cu_2(\mu\text{-}O)_2]^{2+}$ core.[11,13] Laser excitation into the low-energy tail of the latter band (457.9 or 514.5 nm radiation from an argon ion laser) causes resonance enhancement of several features in the Raman spectrum. A large number of Raman peaks are observed, suggesting that many different vibrational modes, including R_3-TACN ring deformations and/or R group vibrations, are coupled to this charge-transfer absorption.[28] To positively identify vibrations involving the $[Cu_2(\mu\text{-}O)_2]^{2+}$ core, the complexes were synthesized using $^{18}O_2$, resulting in double ^{18}O incorporation. Importantly, the RR spectrum of each complex contains at least one intense peak in the 583−616 cm^{-1} region (Table 1) that shifts by 19−27 cm^{-1} with double oxygen isotope substitution, showing that these are due to core modes that involve Cu−O stretching. No bands outside this region shift using $^{18}O_2$. All $[Cu_2(\mu\text{-}O)_2]^{2+}$ complexes exhibit such a band, regardless of steric and electronic properties (Chart 1). Many of the frequency values described above are slightly (~10 cm^{-1}) different from those we originally reported;[2,13,14,16,20,29] the frequencies here should be used in place of the earlier values. For details, see the Experimental Section.

As examples, spectra of frozen acetone solutions of $[(^iPr_3TACN)_2Cu_2(\mu\text{-}O)_2](ClO_4)_2$ and its fully ^{18}O-labeled isotopomer are shown in Figure 2. Features are observed at 577, 590, 606 and 775 (not shown) cm^{-1}, and at 565 and 774 (not shown) in the ^{18}O-substituted analogue. The spectra are similar in various solvents as well as solid samples, except for a band at 713 cm^{-1} due to the O−O stretching vibration of the $\mu\text{-}\eta^2\text{:}\eta^2$-peroxo isomer, which is present in some solvents with some counterions.[16,17,30] The most prominent peak occurs at 590 cm^{-1}, and it shifts to 565 cm^{-1} with ^{18}O substitution, suggesting that it is associated with Cu−O stretching.

Table 1. Position of the $Cu_2(\mu\text{-}O)_2$ Vibration in $[L_2Cu_2(\mu\text{-}O)_2]^{2+}$ Complexes[a]

L	solvent	$\nu(Cu_2(\mu\text{-}O)_2)$ ($^{18}O_2$ frequency) (cm^{-1})	UV/vis (nm)	ref
$^iPr_3TACN$[c]	acetone	590 (565)	420	13, 16[b]
d_3-$^iPr_3TACN$[c]	acetone	587	420	this work
d_{18}-$^iPr_3TACN$[c]	acetone	593	420	this work
d_{21}-$^iPr_3TACN$	acetone	592 (568)	420	this work
$^iPr_3TACN$[d]	THF	589 (567)	324, 448	13[b]
d_{21}-$^iPr_3TACN$[d]	THF	590 (571)	324, 448	this work
Bn_3TACN	acetone	603/595	420	this work
Bn_3TACN	CH_2Cl_2	603/595 (576)	318, 430	13[b]
d_6- Bn_3TACN	CH_2Cl_2	601/592 (573)	318, 430	this work
d_{21}-Bn_3TACN	CH_2Cl_2	594/587 (571)	318, 430	13[b]
$(MeO\text{-}Bn)_3TACN$	CH_2Cl_2	600/590 (571)	316, 436	this work
$(^tBu\text{-}Bn)_3TACN$	CH_2Cl_2	598/588 (571)	318, 436	this work
$(MeOOC\text{-}Bn)_3TACN$	CH_2Cl_2	592/575 (567)	316, 426	this work
$(F_3C\text{-}Bn)_3TACN$	CH_2Cl_2	586/567 (563)	316, 426	this work
$^iPr_2BnTACN$	acetone	586 (563)	436	13[b]
Me_3TACN	CH_2Cl_2	604 (581)	300, 405	15
$1/2\,^iPr_4$-*m*-XY	CH_2Cl_2	584 (561)	320, 430	20[b]
$1/2\,^iPr_4$-*p*-XY	CH_2Cl_2	583 (561)	318, 432	20[b]
$1/2\,^iPr_4$-dtne	CH_2Cl_2	585 (568/561)	316, 414	14[b]
$1/2\,d_{28}$-$^iPr_4$-dtne	CH_2Cl_2	603/586 (569)	316, 414	this work
MePY2	*e*	577 (551)	410	21c
Me_4CHD	*e*	605 (581)	296, 392	15
Me_2Et_2CHD	*e*	610 (587)	306, 401	15
Et_4CHD	*e*	616 (590)	312, 406	15
TMPDA	acetone	608 (582)	406	this work
$^iPr_2$-DACO[f]	CH_2Cl_2	632/591 (588)	330, 438	this work
m-$NO_2PhPyNEt_2$[g]	acetone	607 (580), 584 (570)	404	22
Py|Phe-d_4[f]	acetone	607 (578), 566 (555)	402	23
$^iPr_2$-DACO[f]	CH_2Cl_2	632/591 (588)	330, 438	this work

[a] λ_{ex} = 457.9 nm; T = 77 K. All complexes are ClO_4^- salts, unless otherwise indicated. [b] The frequency here corrects the original report (see Experimental Section). [c] λ_{ex} = 514.5 nm. [d] ClO_4^- or PF_6^- salt. [e] λ_{ex} = 406.7 nm; BArF (MePY2) or $SO_3CF_3^-$ (CHD) salt; solid sample. [f] SbF_6^- salt. [g] λ_{ex} = 406.7 nm; T = 193 K; SbF_6^- salt.

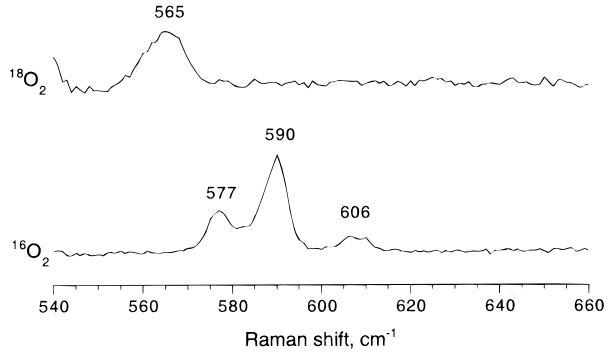

Figure 2. Resonance Raman spectra (λ_{ex} = 514.5 nm) of $[(^iPr_3TACN)_2Cu_2(\mu\text{-}O)_2](ClO_4)_2$ generated from $^{18}O_2$ (top) and from $^{16}O_2$ (bottom) in frozen acetone (77 K).

To aid in the assignment of the other peaks, RR spectra of $[(^iPr_3TACN)_2Cu_2(\mu\text{-}O)_2](ClO_4)_2$ with varying levels of deuteration in the isopropyl groups (d_3 = methine positions; d_{18} = methyl positions; d_{21} = all positions) were measured (Figure 3). It is clear that the peaks at 577 and at 775 cm^{-1} in the undeuterated complex are associated with the isopropyl methyl groups because they are only slightly affected by deuteration of the methine proton (d_3) but shift by 22 cm^{-1} (to ~555 cm^{-1}) and 47 cm^{-1} (to ~728 cm^{-1}), respectively, when the methyl protons are deuterated (d_{18} and d_{21}). The peak at 606 cm^{-1} shifts more gradually upon deuteration, and only by a small amount. Because (a) this peak is only observed in ^{16}O complexes that have a nearby peak from Cu−O stretching, (b) its frequency is too high to involve primarily Cu−N motion,[31] and (c) it is minimally sensitive to deuteration, we assign it as a weakly

(27) Wilkinson, E. C.; Dong, Y.; Zang, Y.; Fujii, H.; Fraczkiewicz, R.; Fraczkiewicz, G.; Czernuszewicz, R. S.; Que, L., Jr. *J. Am. Chem. Soc.* **1998**, *120*, 955−962.

(28) A complete listing of vibrations for all complexes in the 400−900 cm^{-1} region is included in the Supporting Information.

(29) Mahapatra, S.; Halfen, J. A.; Wilkinson, E. C.; Pan, G.; Cramer, C. J.; Que, L., Jr.; Tolman, W. B. *J. Am. Chem. Soc.* **1995**, *117*, 8865−8866.

(30) The solvent/counterion sensitivity is illustrated by the case of $[(^iPr_3TACN)_2Cu_2(\mu\text{-}O)_2]X_2$ in acetone; when X = PF_6 or SbF_6, features due to both $\mu\text{-}\eta^2\text{:}\eta^2$-peroxo− and bis($\mu$-oxo)dicopper cores are observed in UV−vis and RR spectra,[16] but when X = ClO_4, only the bis(μ-oxo)dicopper species is evident at the concentrations used in the RR experiments (Table 1 and Figure 3).[17]

(31) Hathaway, B. J.; Tomlinson, A. A. G. *Coord. Chem. Rev.* **1970**, *5*, 1−43.

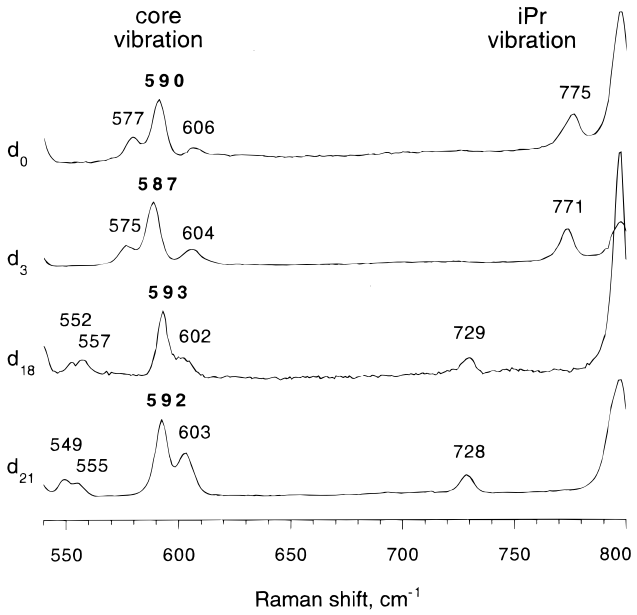

Figure 3. Resonance Raman spectra (λ_{ex} = 457.9 nm) of [(^{i}Pr$_3$TACN)$_2$Cu$_2$(μ-O)$_2$](ClO$_4$)$_2$ in acetone at 77 K (d_0), with the methine protons deuterated (d_3), with the methyl groups deuterated (d_{18}), and with the isopropyl groups completely deuterated (d_{21}). The peaks at 797 cm^{-1} are from acetone solvent.

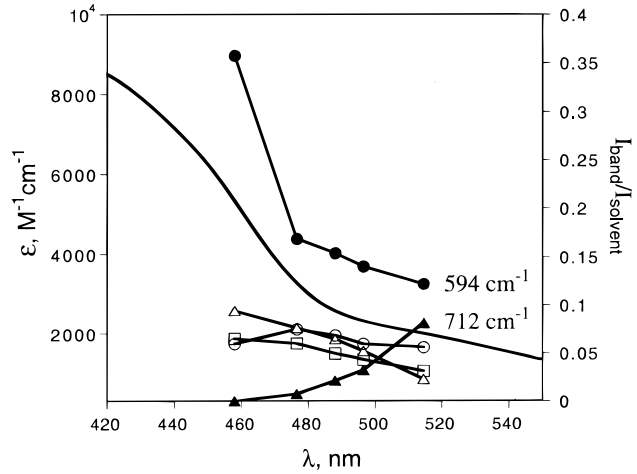

Figure 4. Excitation profile for [(d_{21}-^{i}Pr$_3$TACN)$_2$Cu$_2$(μ-O)$_2$](PF$_6$)$_2$ in acetone, collected as described in the text. The peaks at 594 (●) and 712 cm^{-1} (▲) are due to the [Cu$_2$(μ-O)$_2$]$^{2+}$ core vibration and ν_{O-O} of the (μ-η^2:η^2-peroxo) isomer, respectively. The peaks at 556 (○), 605 (△), and 726 (□) cm^{-1} are due to ligand vibrations. The slight difference between frequencies here and in Figure 3 is due to the difference in counterion.

resonance-enhanced R$_3$TACN ring vibration that "borrows" intensity from the large Cu−O stretching band. The slight frequency shifts observed are also consistent with variable mechanical coupling.

To verify that the resonance enhancements are indeed due to the ~420 nm visible absorption, a partial excitation profile (Figure 4) was measured using [(d_{21}-^{i}Pr$_3$TACN)$_2$Cu$_2$(μ-O)$_2$](PF$_6$)$_2$ in acetone, conditions where UV−vis bands due to both μ-η^2:η^2-peroxo- and bis(μ-oxo)dicopper isomers are present.[16,17,29] The peaks at 556, 594, 605, and 726 cm^{-1} (corresponding to those at 577, 590, 606, and 775 in the undeuterated analog) all gain intensity as the excitation wavelength moves closer to the 420 nm feature in the UV−vis spectrum. The band at 594 cm^{-1} (●) shows the greatest increase in intensity as the excitation

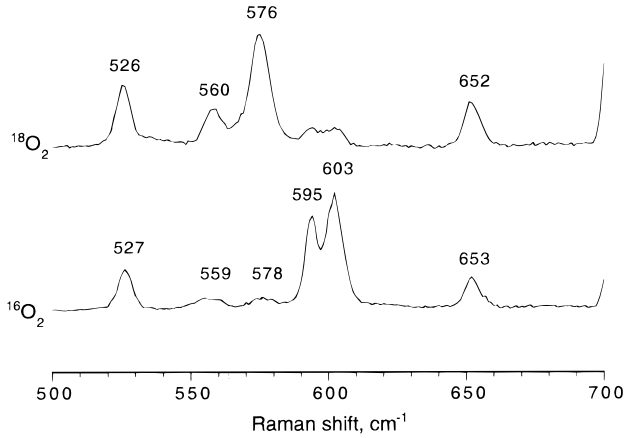

Figure 5. Resonance Raman spectra (λ_{ex} = 457.9 nm) of [(Bn$_3$TACN)$_2$Cu$_2$(μ-O)$_2$](ClO$_4$)$_2$ generated from ^{18}O$_2$ (top) and from ^{16}O$_2$ (bottom) in frozen CH$_2$Cl$_2$ (77 K). The isotope-sensitive doublet centered at 599 cm^{-1} in the lower spectrum is assigned as a Fermi doublet that shifts to 576 cm^{-1} in the upper spectrum.

Table 2. Depolarization Ratios for the Core Vibration(s) in Various [L$_2$Cu$_2$(μ-O)$_2$]$^{2+}$ Complexes in Acetone Solution (T = 193 K)

L	λ_{ex} (nm)	dp ratio
^{i}Pr$_3$TACN	457.9	0.13
Bn$_3$TACN	457.9	0.57, 0.58
TMPDA	406.7	0.21
m-NO$_2$PhPyNEt$_2$	406.7	0.33, 0.35

wavelength approaches λ_{max} for the LMCT transition, consistent with its assignment as a vibration of the [Cu$_2$(μ-O)$_2$]$^{2+}$ core and assignment of the nearby bands at 556 and 605 cm^{-1} as vibrations that involve motion of the R$_3$TACN ligands in the bis(μ-oxo) complexes (see above). The peak at 712 cm^{-1} (▲) is the O−O vibration of the (μ-η^2:η^2-peroxo)dicopper isomer; its intensity increases with longer wavelength excitation, due to the electronic absorption feature of this species at ~510 nm.[32]

Figure 5 shows the RR spectra of frozen CH$_2$Cl$_2$ solutions of the benzyl-appended [(Bn$_3$TACN)$_2$Cu$_2$(μ-O)$_2$](ClO$_4$)$_2$ and its doubly ^{18}O-labeled isotopomer. The spectra of the para-substituted analogues discussed below are all qualitatively similar to this one, in which two bands in the ^{16}O$_2$ complex (603 and 595 cm^{-1}) shift into one band (576 cm^{-1}) in the ^{18}O$_2$ complex. All other features are not sensitive to oxygen isotope substitution but shift drastically with deuterium substitution at the benzylic and aryl positions, showing that they are primarily ligand vibrations. The oxygen isotope-sensitive behavior of the pair of features at ~600 cm^{-1} in all of the Bn$_3$TACN-capped complexes leads us to assign them as a core vibration that is split into a Fermi doublet. In support of this hypothesis, the isotope shifts using the average frequency of the two ^{16}O$_2$ peaks are in the same range as the ^{16}O$_2$−^{18}O$_2$ shifts observed for the other systems (where only a single peak appears for both ^{16}O$_2$- and ^{18}O$_2$-labeled compounds). Moreover, the two peaks have identical depolarization ratios (see Table 2). A combination band from RR bands detected at 291 and 328 cm^{-1} would have roughly the correct sum to be the source of the doublet, a notion that is corroborated by the lack of a doublet for the ^{18}O$_2$ isotopomer, in which the core vibration frequency is farther from

(32) Mahapatra, S.; Halfen, J. A.; Wilkinson, E. C.; Que, L., Jr.; Tolman, W. B. *J. Am. Chem. Soc.* **1994**, *116*, 9785−9786. Note that the O−O vibration in the μ-η^2:η^2-peroxo isomer capped by ^{i}Pr$_3$TACN should be at 713 cm^{-1} (672 cm^{-1} for the ^{18}O$_2$ isotopomer), not 722 cm^{-1} as reported in this reference.

the calculated 619 cm^{-1} combination. Alternatively, the coupling could arise from a Raman-allowed overtone of a nontotally symmetric mode near 300 cm^{-1}; numerous such modes are possible, but our inability to collect low-temperature, low-frequency infrared spectra has prevented evaluation of this possibility.

Resonance Raman Spectroscopy of $[L_2Cu_2(\mu\text{-}O)_2]^{2+}$ Complexes With Bidentate Ligands. Stack and co-workers have reported UV−vis and RR data on a series of bis(μ-oxo)dicopper(III) complexes capped by bidentate alkylated *trans*-1,2-cyclohexanediamine ligands (abbreviated R_4CHD here; R = methyl or ethyl).[15] The RR spectra were qualitatively similar to those described above for TACN complexes in that each had one major band at 610 ± 6 cm^{-1} which shifted by ~25 cm^{-1} when $^{18}O_2$ was used. The commercially available *N,N,N′,N′*-tetramethylpropanediamine (TMPDA) ligand also gives bis(μ-oxo)dicopper(III) complexes that are spectroscopically nearly identical to those with R_4CHD ligands.[33] Bis(μ-oxo)dicopper complexes with bidentate 1,5-diisopropyldiazacyclooctane (^{i}Pr$_2$-DACO) could be prepared similarly: in this case, two bands in the $^{16}O_2$ complex (632 and 591 cm^{-1}) shift into one band in the $^{18}O_2$ complex (588 cm^{-1}). Because the average of the frequencies of the two $^{16}O_2$ peaks is 612 cm^{-1}, very close to the frequencies of the peaks in complexes of other bidentate ligands, these are assigned as a Fermi doublet.

Until this point, all of the $[Cu_2(\mu\text{-}O)_2]^{2+}$ cores had produced only one major ^{18}O-sensitive resonance-enhanced vibration. However, when ligands with two *different* nitrogen donors are used to make bis(μ-oxo)dicopper(III) complexes, two intense oxygen isotope-sensitive bands are observed in the region near 600 cm^{-1} in the low-temperature RR spectrum. The RR spectra of bis(μ-oxo)dicopper complexes with $ArPyNEt_2$ (2-(diethylaminomethyl)-6-arylpyridine; aryl = C_6H_5, *m*-$C_6H_4NO_2$)[22] and with Py|Phe (*N*-ethyl-*N*-(2-phenylethyl)-2-(2-aminoethyl)pyridine)[23] ligands are extremely similar; the former is shown in Figure 6. In each spectrum, there is a large feature at ~607 cm^{-1} which shifts by 28 ± 1 cm^{-1} with $^{18}O_2$ substitution. From these characteristics, it is clearly analogous to the vibrations observed in complexes with CHD, TMPDA, and DACO bidentate ligands. The second vibration is at lower energy (582 or 566 cm^{-1}, respectively) and curiously shifts by a smaller amount (12 ± 2 cm^{-1}) with $^{18}O_2$ substitution.

Additional experiments on the compound with $ArPyNEt_2$ and $PhPyNEt_2$ ligands verify that the unusual second vibration is also due to the bis(μ-oxo)dicopper core. (1) Neither peak is observed in solutions warmed to room temperature to decompose the bis(μ-oxo)dicopper complex. (2) The dependence of RR intensity on excitation wavelength (Figure 6, inset) reveals that both peaks have similar profiles. This shows that the bands are from the same chromophore, or from two compounds with a similar UV−vis feature. (3) Monitoring a solution sample of $[(PhPyNEt_2)_2Cu_2(\mu\text{-}O)_2]^{2+}$ by RR spectroscopy at −70 °C shows that the intensity of both bands decreases over time in an exponential decay. The first-order rate constants are the same for each band (3.6 × 10^{-4} s^{-1}), in reasonable agreement with the rate measured by UV−vis spectroscopy (6 ± 2 × 10^{-4} s^{-1}).[22] Therefore, these bands could only be from different compounds if they coincidentally decompose at the same rate or are in rapid equilibrium. It seems most likely that both vibrations come from the same compound, that a new vibrational feature of the $[Cu_2(\mu\text{-}O)_2]^{2+}$ core has been uncovered, and that its presence is related to the lower symmetry of the bidentate ligand.

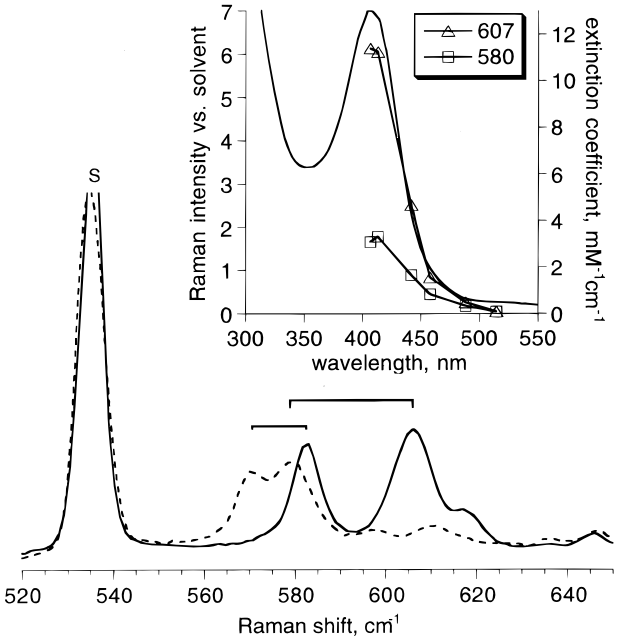

Figure 6. Resonance Raman spectra (λ_{ex} = 457.9 nm) of $[(ArPyNEt_2)_2Cu_2(\mu\text{-}O)_2](SbF_6)_2$ generated from $^{16}O_2$ (—) and from $^{18}O_2$ (− − −) in frozen acetone (77 K). The brackets connect peaks proposed to be from the same mode in different isotopomers. Inset: Excitation profile of $[(ArPyNEt_2)_2Cu_2(\mu\text{-}O)_2](SbF_6)_2$ in acetone solution at −80 °C.

Single Oxygen-Isotope Labeling Experiments. Using "$^{16/18}O_2$" (a statistical mixture of $^{16}O_2$, $^{16}O^{18}O$, and $^{18}O_2$), we synthesized bis(μ-oxo)dicopper cores with a single ^{18}O label. If the ~600 cm^{-1} vibration were not due to the entire core, then the singly labeled compound would appear identical to a superposition of the $^{16}O_2$ and $^{18}O_2$ compounds, while a tetraatomic vibration would give an intermediate frequency. The $[(^iPr_2BnTACN)_2Cu_2(\mu\text{-}O)_2]^{2+}$ and $[(TMPDA)_2Cu_2(\mu\text{-}O)_2]^{2+}$ complexes were chosen as representative complexes with tridentate and bidentate ligation because these had a relatively small number of additional Raman bands in the 550−650 cm^{-1} region. Peak-fitting analysis of RR spectra of samples prepared using $^{16/18}O_2$ showed that a new intermediate band was present in each mixture. Thus, a band in $[(^iPr_2BnTACN)_2Cu_2(\mu\text{-}O)_2]^{2+}$ at 580 ± 2 cm^{-1}, between the $^{16}O_2$ and $^{18}O_2$ peaks at 585 and 562 cm^{-1}, and a band in $[(TMPDA)_2Cu_2(\mu\text{-}O)_2]^{2+}$ at 598 ± 2 cm^{-1}, between the $^{16}O_2$ and $^{18}O_2$ peaks at 608 and 582 cm^{-1}, are assigned to a $Cu_2(\mu\text{-}^{16}O)(\mu\text{-}^{18}O)$ isotopomer. The presence of a new isotopomer in the mixture strongly implies that the core vibration is tetraatomic. (For details, see the Supporting Information.)

Theoretical Studies. As part of an earlier investigation of $[Cu_2(\mu\text{-}O)_2]^{2+}$ complexes, force constants and vibrational frequencies for $[(H_3N)_3Cu(\mu\text{-}O)_2Cu(NH_3)_3]^{2+}$, which models the tridentate ligation of the TACN complexes, were derived from ab initio calculations at the RHF/STO-3G level of theory.[13] These calculations (using idealized C_{2h} symmetry) predicted two oxygen isotope-sensitive vibrations of the core with frequencies of 711 and 693 cm^{-1}, corresponding to modes of A_g and B_g symmetry, respectively.[34] The nature of these will be discussed at length below. The high values of the calculated frequencies relative to those observed experimentally are not unexpected

(33) Our data on complexes with the TMPDA ligand agree with those recently presented with the analogous perchlorate salt: Mahadevan, V.; DuBois, J. L.; Hedman, B.; Hodgson, K. O.; Stack, T. D. P. *J. Am. Chem. Soc.* **1999**, *121*, 5583−5584.

(34) In ref 13, these frequencies were scaled by a factor of 0.89 to account for systematic errors in RHF calculations.[35]

Chart 2

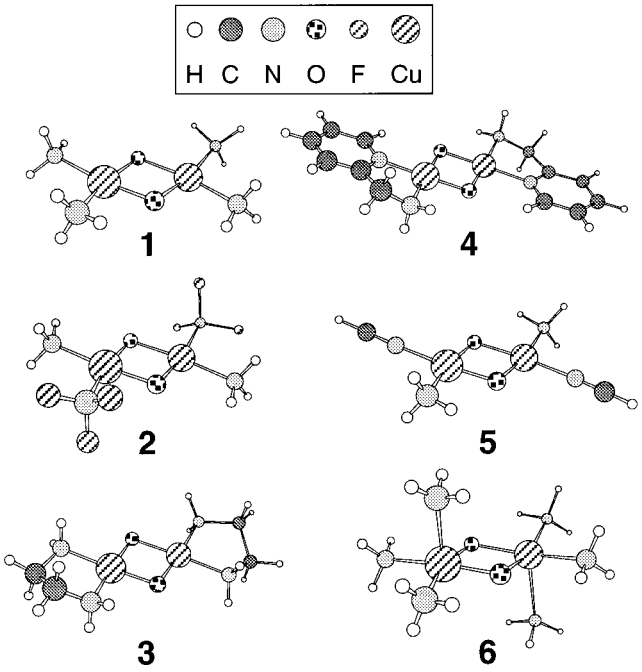

Table 3. Geometrical and Raman Parameters Calculated (BPW91/pVDZ) for Different $[Cu_2(\mu\text{-}O)_2]^{2+}$ Cores

molecule	point group	r_{Cu-O} (Å)	Raman frequency (cm^{-1})[a]	isotope shift (cm^{-1})	dp[a]	nature of mode
1	D_2	1.830	577.8(553.3)	24.5	0.75	B_1, pairwise
			578.7(554.1)	24.6	0.11	A, breathing
2	C_i	1.809	587.0(560.3)	26.7	0.38	A_g, pairwise
		1.812	604.0(579.3)	24.7	0.12	A_g, breathing
3	D_2	1.825	573.5(553.3)	20.2	0.75	B_1, pairwise
			594.4(569.4)	25.0	0.11	A, breathing
4	C_i	1.823	565.6(541.5)	24.1	0.43	A_g, pairwise
		1.827	598.6(570.1)	28.5	0.15	A_g, breathing
5	C_{2h}	1.805	588.1(563.8)	24.3	0.29	A_g, long Cu−O str.
		1.822	603.8(576.5)	27.3	0.23	A_g, short Cu−O str.
6	C_{2h}	1.849	543.5(520.5)	23.0	0.10	A_g, breathing
			547.3(524.3)	23.0	0.75	B_g, pairwise

[a] Reported as $^{16}O_2$ ($^{18}O_2$). Frequency and isotope shift in cm^{-1}, depolarization ratios (dp) are unitless.

because calculations at the Hartree−Fock level typically overestimate frequencies by 10−15%.[35] Those calculations have been repeated here using density functional theory (DFT) at the BPW91/pVDZ level, which is known to provide high accuracy for vibrational frequencies in a wide variety of chemical structures.[36] In particular, six systems are chosen to maximize opportunities for comparison between high- and low-symmetry ligand environments, between bidentate and tridentate capping ligands, and between theoretical and experimental models. As illustrated in Chart 2, the theoretical model systems are $[(NH_3)_2Cu_2(\mu\text{-}O)_2]^{2+}$ (**1**), $[(NH_3)_2(NF_3)_2Cu_2(\mu\text{-}O)_2]^{2+}$ (**2**), $[(1,2\text{-diaminoethane})_2Cu_2(\mu\text{-}O)_2]^{2+}$ (**3**), $[(2\text{-(aminomethyl)pyridine})_2Cu_2(\mu\text{-}O)_2]^{2+}$ (**4**), $[(NH_3)_2(HCN)_2Cu_2(\mu\text{-}O)_2]^{2+}$ (**5**), and $[(NH_3)_6Cu_2(\mu\text{-}O)_2]^{2+}$ (**6**). Aspects of models **1**[18d,21c] and **6**,[11b,13,18,29] unrelated to their Raman spectra have been investigated previously at various levels of electronic structure theory (see Table 3). Optimized structures for all six models are available as Supporting Information.[37] In each case, only two Raman-active vibrations involved substantial oxygen atom motion and thus would be expected to show isotope shifts in RR spectra. The symmetry, assignment, and trends in these vibrations will be addressed below in the Discussion section.

Table 4. Core Interatomic Distances (Å) for Different Electronic States of **2**

bond length	electronic state ^1A_g	electronic state ^3A_u
Cu−Cu	2.800	3.059
O−O	2.295	2.205
Cu−O(1)	1.809	1.878
Cu−O(2)	1.812	1.892

To gain insight into resonance Raman intensities, which depend on differences in geometry between the ground and excited states, configuration interaction calculations including all single excitations (CIS) from a restricted Hartree−Fock reference were carried out for **2**. At the CIS/pVDZ level, the first state showing significant oscillator strength (0.465) is predicted to be a ^1A_u state well described as a one-electron excitation from the HOMO to the LUMO. Since an RHF reference and subsequent CIS treatment of this system would be expected to perform poorly for all but the most qualitative information, we do not analyze this calculation for energetic data. However, to approximate the structure of the excited state, we have optimized the structure of the corresponding *triplet* of **2** at the BPW91/pVDZ level (DFT is not well suited to handling the open-shell singlet excited state, as it is multi-determinantal; however, the corresponding triplet does not suffer from this complication, and we expect the triplet structure to be similar to that of the singlet). The HOMO → LUMO electronic excitation causes a significant shift in the core structure, with the O−O bond shortening by 0.090 Å and the Cu−Cu distance increasing by 0.259 Å (Table 4). A somewhat larger asymmetry in the two Cu−O bond lengths compared to that in the ground state is also observed. Thus, interestingly, electronic excitation causes the core to distort in the direction of creating a $Cu_2(\mu\text{-}\eta^2\text{:}\eta^2\text{-}O_2)$ structure.

Discussion

When complexes containing the bis(μ-oxo)dicopper(III) core were irradiated in their charge-transfer bands at 390−450 nm, intense RR bands were observed. Near 600 cm^{-1}, at least one extremely intense band was invariably present, serving as a signature for the presence of this core. In cases where multiple bands were evident, ^{18}O substitution often led to the assignment of multiple bands as Fermi doublets because two bands with one isotopomer corresponded to only one band with the other isotopomer. Finally, partial isotopic labeling and calculations confirmed that this vibration involves movement of all four core atoms.

Trends in the Frequency of the $[TACN_2Cu_2(\mu\text{-}O)_2]$ Vibration Indicate That It Couples with Ligand Modes. We have pointed out the presence of Fermi doublets, the sensitivity of the core frequency to deuterium substitution on the $^iPr_3TACN$ ligand, and the fact that the $^{16}O-^{18}O$ isotope shift for the core frequency with TACN ligands was invariably less than the amount expected for a Cu−O oscillator (28 cm^{-1}). Each of these observations suggests that ligand vibrations are coupled to the "core vibration" in the normal mode responsible for the intense ~600 cm^{-1} band.

(35) Pople, J. A.; Scott, A. P. Wong, M. W.; Radom, L. *Isr. J. Chem.* **1993**, *33*, 345−350.

(36) Scott, A. P.; Radom, L. *J. Phys. Chem. A* **1996**, *100*, 16502−16513.

(37) It appears that equilibrium structure **5** is only very weakly stable, because several initial attempts at optimization converged smoothly to a $Cu_2(\mu\text{-}\eta^2\text{:}\eta^2\text{-}O_2)$ core. This observation is consistent with the notion that weak donors (like acetonitrile) fail to stabilize the copper(III) oxidation state as effectively as strong donors and thus destabilize the $Cu_2(\mu\text{-}O)_2$ core.

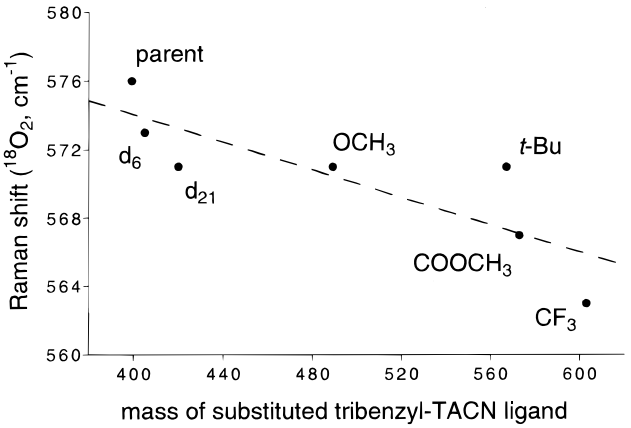

Figure 7. Plot of the frequency of the $Cu_2(\mu\text{-}O)_2$ vibration in $[((p\text{-}X{-}C_6H_4CH_2)_3TACN)_2Cu_2(\mu\text{-}^{18}O)_2](ClO_4)_2$ vs the mass of the ligand.

Table 1 includes several bis(μ-oxo)dicopper complexes with *para* substituents on the benzyl rings of $[(X\text{-}Bn_3TACN)_2Cu_2(\mu\text{-}O)_2]^{2+}$ (X = MeO, *t*-Bu, MeO_2C, and CF_3),[19a] which can be used to examine the reasons for the shifts in the core frequency. For simplicity, the following discussion uses the frequencies measured under identical conditions for the $[(X\text{-}Bn_3TACN)_2Cu_2(\mu\text{-}^{18}O)_2]^{2+}$ isotopomers, in which the $Cu_2(\mu\text{-}O)_2$ peaks are singlets. The core vibration frequency and the electron-withdrawing or electron-donating nature of the substituents do not appear to be related, but a correlation (R = 0.84) is observed when the core vibration frequency is compared to the mass of the ligand (Figure 7). The decrease in frequency of the core mode with heavier benzyl substituents suggests that the $Cu_2(\mu\text{-}O)_2$ vibration and Cu−N and/or ligand vibrations [e.g., N−C(benzyl) stretches] are coupled. In support of this ligand mass effect on the core mode, a smooth decrease in the $Cu_2(\mu\text{-}O)_2$ frequency with the extent of benzyl group deuteration (d_6 = benzylic positions, and d_{21} = all positions) is apparent. This result is not general, however, as deuteration of the isopropyl groups in complexes of ^{i}Pr$_3$TACN or ^{i}Pr$_4$dtne did not cause systematic changes in the frequency of the $Cu_2(\mu\text{-}O)_2$ vibration. This difference between the behavior of the isopropyl- and X-benzyl-substituted ligands presumably reflects a change in ligand vibrational coupling with the core, but it has not yet been possible to determine the reason for this change.

In the X-ray structures of $[(Bn_3TACN)_2Cu_2(\mu\text{-}O)_2]^{2+}$ and $[(^iPr_4dtne)Cu_2(\mu\text{-}O)_2]^{2+}$ there are unusually short distances between ligand benzylic or isopropyl methine protons and the bridging oxo groups that are consistent with ground-state C−H···O hydrogen bonding interactions in the crystals.[13,14] These interactions are of interest because they may reside on the potential energy surface for the scission of these C−H bonds by the oxo groups during the intramolecular decomposition reactions of the $[Cu_2(\mu\text{-}O)_2]^{2+}$ complexes.[19a] Hydrogen bonding of this type could be manifested in the RR spectrum as a shift in the core vibration upon selective replacement of the hydrogen in question by deuterium.[38] However, the data in Table 1 show that in each case, deuteration at the position α to the nitrogen donor gives a core frequency intermediate between those of complexes with undeuterated and totally deuterated substituents, implying that the cause of the shift in the core vibration does not involve a localized interaction such as C−H···O hydrogen bonding. These results suggest that this hydrogen bonding either does not exist or does not cause detectable RR shifts under the frozen solution conditions of our experiments. Thus, mass influences from the entire organic substituent cause the effects on the core vibration, apparently from a contribution from Cu−N stretching in the $Cu_2(\mu\text{-}O)_2$ mode.

The Effect of Coordination Number. The $[Cu_2(\mu\text{-}O)_2]^{2+}$ frequencies are systematically higher (by ~20 cm^{-1}) for complexes that have two-coordinate ligands than for those with three-coordinate R_3TACN ligands. Recent theoretical work by Alvarez and co-workers has shown that bis(μ-oxo)dicopper complexes are stabilized when the equatorial ligands can reside closer to the $Cu_2(\mu\text{-}O)_2$ plane (as expected for a d^8-Cu^{III} complex).[18b] Thus, it is possible that the lesser constraints of the bidentate ligands allow the $[Cu_2(\mu\text{-}O)_2]^{2+}$ core to relax into a lower-energy square-planar conformation with stronger Cu−O bonds and a correspondingly higher frequency core vibration. Alternatively, the well-known shortening of metal−ligand bonds with decreasing coordination number could cause stronger Cu−O bonding in the complexes with bidentate nitrogen ligands. It should be noted, however, that the energetics of bis(μ-oxo)-dicopper complexes are affected substantially by subtle changes in ligand properties, solvent, and/or counterions;[2,16,17] such "environmental" influences may also contribute to the changes in the copper−oxygen bonding apparently reflected by the trends in core vibration frequencies. This issue will be addressed below using theoretical methods.

Assigning the Experimentally Observed Core Vibrations. When bidentate ligands with two different donors (hereafter, "asymmetric" ligands) were used, two vibrations were present in the characteristic ~600 cm^{-1} region for each isotopomer, and further experiments suggested that two independent modes of the same $[Cu_2(\mu\text{-}O)_2]^{2+}$ core are observable.

Group theory gives insight into the reasons for this difference. The point group to which a specific $M_2(\mu\text{-}O)_2$ core belongs depends on the symmetry of the capping ligands. If there is a symmetric bidentate ligand on each metal, then the core would have D_{2h} symmetry; with asymmetric bidentate ligands disposed in a pseudo-trans (anti) fashion, the symmetry is reduced to C_{2h} (with the C_2 axis perpendicular to the core). The irreducible representations of the four core stretching vibrations are shown in Figure 8, with Raman-allowed vibrations in bold type.[39] Much of the following discussion will involve the first two modes: in the first, labeled "breathing," all four bonds stretch in phase, and in the second, labeled "pairwise," adjacent bonds stretch out of phase.

The most important result of lowering the symmetry to C_{2h} in complexes with "asymmetric" ligands is that the pairwise vibration changes from B_g to A_g. What effect should this change in symmetry have on the RR spectra of $[L_2Cu_2(\mu\text{-}O)_2]^{2+}$ species? The major contributor to resonance enhancement, *A*-term scattering, is only available to totally symmetric modes.[40] In the symmetric CHD, TMPDA, and DACO-capped complexes, only the breathing mode in Figure 8 is of A_g symmetry, while in the asymmetric ArPyNEt$_2$ and Py|Phe complexes, *both* breathing and pairwise modes have an A_g representation. This provides a ready explanation for the number of oxygen isotope-sensitive bands in the complexes with each kind of bidentate ligand. Comparison of frequencies with symmetric and asymmetric bidentate ligands suggests that the consistently observed band around 610 cm^{-1} is the omnipresent breathing vibration, while the new pairwise vibration is the one at lower energy in the ligands with an asymmetric donor set. TACN-ligated

(38) Shiemke, A. K.; Loehr, T. M.; Sanders-Loehr, J. *J. Am. Chem. Soc.* **1986**, *108*, 2437−2443.

(39) In this simple analysis, we only consider the linear combinations of the four Cu−O stretches, even though the bare Cu_2O_2 core has a total of six normal modes. See the Appendix for details and discussion.

(40) Clark, R. J. H.; Dines, T. J. *Angew. Chem., Int. Ed. Engl.* **1986**, *25*, 131−158.

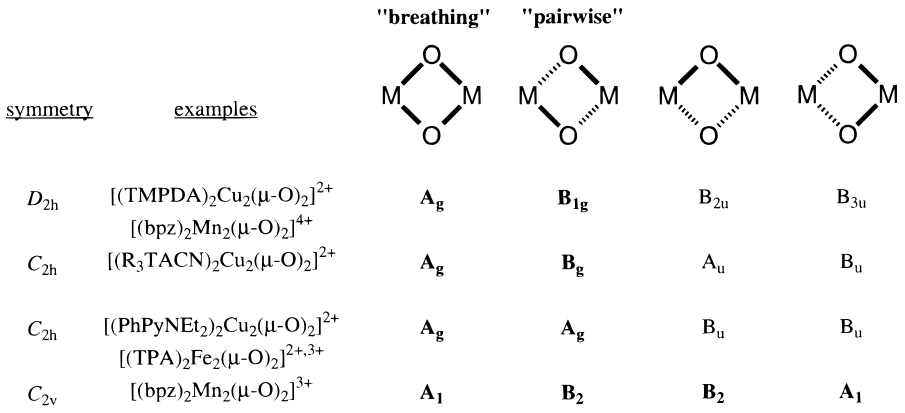

Figure 8. Normal modes of the $[M_2(\mu\text{-}O)_2]^{n+}$ core, with symmetry and polarization labels for various symmetries.[41] Solid and dashed lines represent stretching bonds and contracting bonds, respectively, and boldface labels indicate that these modes have Raman-allowed symmetries.

complexes have axial substituents which lower the symmetry to C_{2h} (with the C_2 axis through the oxygen atoms),[41] but the irreducible representations of the core vibrations in this orientation of this point group are similar to those in D_{2h} symmetry. Again, only the breathing vibration has the appropriate A_g symmetry for resonance enhancement, corresponding with the single major isotope-sensitive vibration.

Depolarization ratios ($\rho = I_\perp/I_{||}$) can be used to assign the symmetries of Raman vibrations. This ratio ρ is expected to be 0.75 for nontotally symmetric vibrations, and less than 0.75 for totally symmetric vibrations (in most cases, A_g).[42] The generally low values for the core modes in complexes with various capping ligands (Table 2) are consistent with an assignment of all intense vibrations as totally symmetric. Thus the single bands for the D_{2h} TACN and TMPDA complexes correspond to the core breathing mode. Only when the symmetry is lowered to C_{2h} is the pairwise mode totally symmetric and thus resonance-enhanced.

Similar symmetry effects have been observed in the Cu−O vibrations of (μ-η^2:η^2-peroxo)dicopper(II) complexes. In the model compound $[(HB(3,5\text{-}Ph_2pz)_3)_2Cu_2(\mu\text{-}\eta^2\text{:}\eta^2\text{-}O_2)]$, normal coordinate analysis was used to identify a RR peak at 284 cm^{-1} as the A_g Cu_2O_2 breathing mode. The B_{1g} pairwise mode was not resonance-enhanced in these spectra (although an overtone of this vibration was observed because first overtones are always totally symmetric).[43] However, when the symmetry of the site is reduced by its surroundings, as in the active site of the oxy form of the protein hemocyanin, both breathing and pairwise modes are observable.[44] This is directly analogous to the situation in the above bis(μ-oxo)dicopper(III) complexes, in which symmetry reduction results in a greater number of vibrations becoming totally symmetric.

Theoretical Characterization of $[Cu_2(\mu\text{-}O)_2]^{2+}$ Core Distortions and Vibrations. The ground-state Cu−O bond lengths in the optimized theoretical models may be found in Table 3. In the asymmetric cores of **2** and **4**, the difference between the two distinct Cu−O bond lengths is no more than 0.004 Å; in **5**, where there is a large difference in donating ability between the sp lone pair of HCN and the sp^3 lone pair of ammonia, the Cu−O bond length difference is a more substantial 0.017 Å. Table 3 also provides details on two Raman-active core vibrations found in theoretical models **1**−**6** (Chart 2) that are proposed to correspond to those assigned experimentally, namely, a symmetric breathing mode (always of A or A_g type symmetry) and a pairwise mode (of varying symmetry depending on the specific structure).

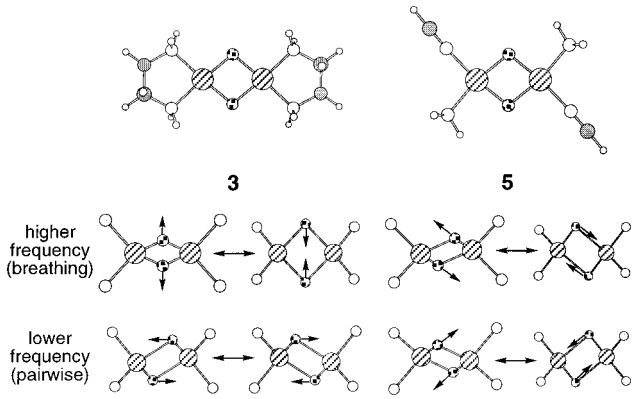

Figure 9. Illustrations of the key rhomb normal modes computed at the BPW91/pVDZ level for **3** and **5**, shown as the two extremes of atom displacement. In each case, the lower frequency mode appears below and the higher frequency mode above; each set of two is immediately below the relevant molecule. Carbon and hydrogen atoms have been removed for clarity in the normal mode depictions, but the orientation remains that shown for the full molecule.

Figure 9 indicates how the character of these normal modes changes when the core symmetry is changed. In the case of **3**, which has equivalent Cu−O bond lengths, the normal modes agree closely with the idealized breathing and pairwise vibrations in Figure 8. More specifically, the breathing mode (top) involves simultaneous motion of all four rhomb atoms in and out along the vectors connecting them to the center of the rhomb, while the pairwise (bottom) mode involves primarily side-to-side motions of the oxygen atoms and has little contribution from copper. We emphasize that the motion of the oxygen atoms is either parallel to the copper−copper vector (pairwise mode) or perpendicular to it (breathing mode). In the very asymmetric case of **5**, on the other hand, the motions of the oxygen atoms in each mode have effectively been rotated by about 45°. Thus, the high-frequency mode (top) essentially consists of the symmetric stretching of the shorter Cu−O bonds (with the longer Cu−O bonds showing little variation), while the low frequency mode (bottom) stretches only the longer Cu−O bonds (with the shorter Cu−O bonds showing little variation). Model

(41) Although the core geometries of both $[(R_3TACN)_2Cu_2(\mu\text{-}O)_2]^{2+}$ and $[(PhPyNEt_2)_2Cu_2(\mu\text{-}O)_2]^{2+}$ complexes belong to the point group C_{2h}, the C_2 axis is in the $Cu_2(\mu\text{-}O)_2$ plane in the former but perpendicular to the $Cu_2(\mu\text{-}O)_2$ plane in the latter, causing the same pairwise vibration to have a B_g representation in the former and an A_g representation in the latter.

(42) Strommen, D. P. *J. Chem. Educ.* **1992**, *69*, 803−807.

(43) Baldwin, M. J.; Root, D. E.; Pate, J. E.; Fujisawa, K.; Kitajima, N.; Solomon, E. I. *J. Am. Chem. Soc.* **1992**, *114*, 10421−10433.

(44) Ling, J.; Nestor, L. P.; Czernuszewicz, R. S.; Spiro, T. G.; Fraczkiewicz, R.; Sharma, K. D.; Loehr, T. M.; Sanders-Loehr, J. *J. Am. Chem. Soc.* **1994**, *116*, 7682−7691.

system **4** shows slight asymmetry in the rhomb, and the normal modes are intermediate between the two extremes illustrated for **3** and **5** (see Supporting Information for details). In general, it seems likely that a continuum exists between the high- and low-symmetry extremes, and the position of any given system along that continuum will be strongly influenced by the nature of the ligands.

Although the observed breathing mode predicted for **6** is 50−60 cm^{-1} less than the experimental value for compounds with TACN ligands, the isotope shift of 23 cm^{-1} is quantitatively reproduced. This illustrates that, particularly for such low-frequency modes, one should exercise caution in comparing the absolute values from simple, gas-phase theoretical models to experimental systems involving more complex ligands, counterions, and condensed-phase effects. With this *caveat* in mind, however, we now compare various aspects of the theoretical models one to another in order to understand specific changes occurring for different choices of ligand environments. We note that for the theoretical and experimental structures that are most closely comparable, namely **4** and $[(ArPyNEt_2)_2Cu_2(\mu\text{-}O)_2]^{2+}$, the predicted and observed frequencies are, respectively, 566 and 584 cm^{-1} for the pairwise mode and 599 and 607 cm^{-1} for the breathing mode, which is reasonably good agreement given the remaining differences between the two systems.

First, we consider the effects of bidentate vs tridentate ligands. A comparison of **1** to **6**, in which the coordination number is changed using the same type of ligand, indicates that (a) force constants in the rhomb are larger in the bidentate case, (b) the frequency of the breathing mode is similar to the frequency of the pairwise mode in each system, and (c) oxygen isotope effects on either mode in either system are nearly equivalent. Point (a) indicates that the lower frequencies observed for tridentate ligands vs bidentate ligands are indeed ascribable to out-of-plane distortions of equatorial ligands (in **6** the $N_{eq}-Cu-O-Cu$ dihedral angle is 168.6°, while in **1** it is 179.6°)[18b] and/or coordination number effects. Thus, the theoretical results support stronger Cu−O bonding in the cores with a lower-coordinate copper atom.

Point (b) does not imply that an asymmetric ligand environment is necessary for significant differences in energy between the pairwise and breathing modes, because in **3**, in which the nitrogen lone pairs are equivalent and the symmetry is identical to **1**, the energy difference between the two modes is 20.9 cm^{-1}. This latter difference is similar to that found in **2**, 17.0 cm^{-1}, where both nitrogen ligands donate sp^3 lone pairs of different Lewis basicity, and smaller than that found for **4**, 33.0 cm^{-1}, where one nitrogen ligand donates an sp^2 lone pair and the other an sp^3 lone pair. In the limit of a highly asymmetric ligand environment, as present in **5**, it no longer makes sense to refer to breathing and pairwise modes, as already noted above, since the bond stretching modes are effectively localized. Thus it is difficult to deconvolute the effect of asymmetric ligands on the frequencies of the breathing and pairwise modes from the change in localization of these normal modes, and it is not possible to draw a simple correlation between the difference between the two core frequencies and the asymmetry of the ligand environment.

With respect to isotope shifts, point (c), the computed values for the breathing modes of **1**−**5** are in very good agreement with values observed in the experimental systems, for the most part covering a range of 25−29 cm^{-1}. In the two experimental cases where the pairwise mode is observed, the measured isotope effect is considerably smaller: 14 cm^{-1} for $[(ArPyNEt_2)_2Cu_2(\mu\text{-}O)_2]^{2+}$ and 11 cm^{-1} for $[(Py|Phe)_2Cu_2(\mu\text{-}O)_2]^{2+}$. For **4**, the theoretical model most closely related to these two, the oxygen isotope effect *is* predicted to be smaller for the pairwise mode than for the breathing mode, but only by 4.4 cm^{-1}, not as much as the ∼16 cm^{-1} observed in the experimental systems. Comparison to the other theoretical models suggests, however, that this too is an observable that is very sensitive to ligand participation in the normal mode and/or environmental effects. In **3** the isotope effect is also predicted to be smaller for the pairwise mode than for the breathing mode, in **1** and **6** there is predicted to be no difference, and in **2** the isotope effect is predicted to be *larger* for the pairwise mode. Thus, as in the experimental results, there is variable ligand coupling with the core modes which is difficult to generalize.

Resonance Raman intensities are proportional to the square of the normal mode displacements required to convert from the ground- to excited-state structure.[45] In an effort to rationalize the experimentally observed RR intensities for the pairwise and breathing modes in asymmetric bidentate dicopper complexes (where both are active), we expressed the difference in the equilibrium structures for triplet **2** and ground-state (singlet) **2**, obtained as described above, in the basis of the normal modes of the latter. Least-squares fitting indicates that the breathing and pairwise mode eigenvectors (expressed in mass-scaled Cartesian coordinates) have coefficients of 0.26 and 0.27, respectively, suggesting that roughly equal intensities might be expected for these modes in a RR experiment. The standard error from the fit is large, however, at 0.16 and 0.17, respectively. Thus, operating under the assumption that the geometry of the lowest-energy triplet well represents the open-shell singlet which is accessed by long-wavelength UV absorption and has the same spatial electronic symmetry, theory provides support for the notion that the pairwise and breathing modes should have similar intensities in RR experiments. However, it is not possible to provide more quantitative estimates of those intensities relative to one another.

Comparison to $[Fe_2(\mu\text{-}O)_2]^{n+}$ ($n = 2, 3$) and $[Mn_2(\mu\text{-}O)_2]^{n+}$ ($n = 3, 4$) Cores. The $[Fe_2(\mu\text{-}O)_2]^{2+,3+}$ cores of a series of model compounds with tris(2-pyridylmethyl)amine (TPA) capping ligands have been examined in detail, structurally by EXAFS,[9,10] X-ray crystallography,[10,46] and theoretical calculations,[47] and vibrationally by resonance Raman spectroscopy.[27] The best-studied $Fe^{III}Fe^{IV}$ compound has a valence-delocalized core, with each equivalent iron atom bearing a formal charge of +3.5.[10,27] Intriguingly, the structures of Fe^{III}_2 and $Fe^{III}Fe^{IV}$ complexes have asymmetric cores with two longer Fe−O bonds and two shorter Fe−O bonds, disposed in a pairwise fashion with the long bonds across from each other (similar to those of the lowest structures shown in Figure 9). Because there is an amine trans to one oxo bridge and a pyridine trans to the other oxo bridge in $[L_2Fe_2(\mu\text{-}O)_2]^{n+}$, this distortion may be related to the trans influences of the two different kinds of nitrogen donors. Only one of the two A_g Fe−O bond stretching modes (Figure 8) had a large intensity in the RR spectrum, and single isotopic labeling was more consistent with its assignment as a mode like the pairwise mode in the copper system described above.[27] However, it is important to note that the ground-state asymmetry of these $[Fe_2(\mu\text{-}O)_2]^{n+}$ cores ($\Delta r_{Fe-O} \approx 0.06$ Å)[9,10] probably changes the nature of the vibrations labeled "breathing" and "pairwise" above such that they correspond to stretching the stronger and

(45) (a) Johnson, B. B.; Peticolas, W. L. *Annu. Rev. Phys. Chem.* **1976**, *27*, 465−491. (b) Warshel, A. *Annu. Rev. Biophys. Bioeng.* **1977**, *6*, 273−300. (c) Clark, R. J. H.; Stewart, B. *Struct. Bond.* **1979**, *36*, 1−80.

(46) Zheng, H.; Zang, Y.; Dong, Y.; Young, V. G., Jr.; Que, L., Jr. *J. Am. Chem. Soc.* **1999**, *121*, 2226−2235.

(47) Ghosh, A.; Almlöf, J.; Que, L., Jr. *Angew. Chem., Int. Ed. Engl.* **1996**, *35*, 770−772.

weaker pairs of Fe−O bonds, like the modes for theoretical model **5** in Figure 9. Finally, it is noteworthy that the frequencies of the core vibrations in the copper compounds described above are more than 60 cm^{-1} lower than those in the iron compounds, perhaps reflecting a difference in bond strengths.

Dinuclear manganese compounds with high-valent $[Mn_2(\mu\text{-}O)_2]^{n+}$ cores are much more thermally stable than their iron and copper analogues and have consequently been characterized more often by X-ray crystallography.[8] The $[Mn_2(\mu\text{-}O)_2]^{4+}$ core containing two Mn^{IV} ions is usually symmetric with nearly equivalent Mn−O bond lengths and thus is comparable to the symmetric bis(μ-oxo)dicopper compounds above (idealized D_{2h} symmetry). In the only report we know of RR spectra for a compound containing this $Mn^{IV}{}_2$ core, one intense polarized oxygen-isotope sensitive band was observed at 693 cm^{-1} in $[(pbz)_4Mn_2(\mu\text{-}O)_2]^{4+}$ (bpz = 2-(2-pyridyl)benzimidazole).[25] Its assignment as the A_g breathing mode is directly analogous to the assignment of the major band in the TACN-capped bis(μ-oxo)dicopper complexes.

Resonance Raman spectroscopy has also been applied to compounds with mixed valence $[Mn_2(\mu\text{-}O)_2]^{3+}$ cores in an attempt to discern a spectroscopic signature for potential intermediates in catalase and the oxygen-evolving complex of photosystem II.[24,26] Interestingly, up to four oxygen-isotope sensitive vibrations were present in the spectra of $[(L)_4Mn_2(\mu\text{-}O)_2]^{3+}$ in the range 550−700 cm^{-1} (L = pbz, bpy, phen).[26] Why were there more vibrations than in the analogous $[Fe_2(\mu\text{-}O)_2]^{3+}$ complex? The key is that these $Mn^{III}Mn^{IV}$ bis(μ-oxo) complexes, unlike the $Fe^{III}Fe^{IV}$ bis(μ-oxo) complex described above, are valence-localized. Thus, the symmetry is lowered from D_{2h} to C_{2v} and all four core stretching vibrations are Raman-allowed (Figure 8), although one would expect only the two totally symmetric A_1 vibrations to acquire substantial RR intensity. Clearly, more data are necessary to understand the vibrations of these complicated, yet interesting, bis(μ-oxo)dimanganese clusters.

Conclusions

In addition to assigning several peaks in the 500−900 cm^{-1} region of the resonance Raman spectra of triazacyclononane-supported bis(μ-oxo)dicopper complexes, this work firmly establishes that the presence of a characteristic vibration near 600 cm^{-1} is common to all known complexes containing the $[Cu_2(\mu\text{-}O)_2]^{2+}$ core. Several independent pieces of evidence now support its assignment as the A_g-symmetry breathing mode. First, the sensitivity of the feature to ^{18}O-substitution proves that it involves the bridging oxo groups, although the small magnitude of some of the shifts implicates mixing with Cu−N or ligand vibrations. The resonance enhancement observed upon irradiation into the intense charge-transfer absorption band further corroborates attribution of both the UV−vis and ^{18}O-sensitive RR features to the $[Cu_2(\mu\text{-}O)_2]^{2+}$ core. The ∼600 cm^{-1} Raman feature is polarized and greatly enhanced by the resonance effect, consistent with its being due to a totally symmetric A_g mode.

With none of the symmetric ligands is it possible to see the B_g pairwise core vibration, because it is not subject to *A*-term resonance enhancement. Although an overtone of the pairwise mode disclosed the frequency of this vibration in a symmetric $(\mu\text{-}\eta^2\text{:}\eta^2$-peroxo)dicopper(II) complex,[43] our attempts to locate totally symmetric overtones of the B_g core vibrations in RR spectra of symmetric bis(μ-oxo)dicopper complexes have failed. However, when ligands with two different kinds of nitrogen donors are used, the pairwise vibration acquires resonance enhancement. The observation of this second core vibration, and the agreement with theoretical results, strengthen these assignments. Further, a systematic theoretical study of the effect of the electronic properties of the capping ligands presented here has enabled us to (a) examine the structural and vibrational effects of gradually destroying ligand symmetry, (b) make a preliminary investigation into excited-state distortions of the core, and (c) determine that the increase in Cu−O force constant with lower coordination number can be rationalized without including solvent or environmental factors. Finally, a simple group-theory analysis of the cores rationalizes the number of bands observed in RR spectra of bis(μ-oxo)dimetal complexes of copper, iron, and manganese, showing that similar principles can be used to understand a variety of cores. Such ideas will be useful in the application of resonance Raman spectroscopy to biological systems that may contain a bis(μ-oxo)dimetal unit.

Experimental Section

General Considerations. Tetramethyl-1,3-propanediamine was degassed and dried over activated 3 Å sieves. The syntheses of the copper(I) complexes used here have been described in earlier publications.[13,14,16,19a,20,22,23,29,32] $[(d_6\text{-}Bn_3TACN)Cu(NCMe)](ClO_4)$ was synthesized in a fashion analogous to that reported for $[(Bn_3TACN)Cu(NCMe)](ClO_4)$.[13] The d_2-benzyl chloride was synthesized by reduction of benzoic acid with lithium aluminum deuteride, reaction of the resultant d_2-benzyl alcohol with thionyl chloride, and vacuum distillation. Deuteration of the ligand was verified by GC/MS and ^1H NMR spectroscopy. Copper(I) complexes were handled under a nitrogen atmosphere. Samples using $^{16}O_2$ were prepared by bubbling dioxygen through a solution of the copper(I) complex (5−10 mg in 0.3−1 mL solvent) in a 10-mL Schlenk tube at −80°C. Samples with $^{18}O_2$ were prepared by condensing roughly 10 mL of $^{18}O_2$ gas (Cambridge or Icon, 95−98%) into a 10-mL Schlenk flask containing a frozen (77 K) solution of the copper(I) compound, followed by warming to −80 °C for 10−15 min.

Resonance Raman Spectroscopy. Resonance Raman spectra were collected on a Spex 1403 double spectrometer interfaced with a Spex DM3000 data system, or on an Acton 506 spectrometer using a Princeton Instruments LN/CCD-1100-PB/UVAR detector and ST-1385 controller interfaced with Winspec software. A Spectra-Physics 2030−15 argon ion laser with a power of roughly 40 mW at the sample was employed to give the excitation at 514.5 or 457.9 nm. The spectra were obtained at 77 K using a 135° backscattering geometry. Samples were frozen onto a gold-plated copper coldfinger in thermal contact with a Dewar flask containing liquid nitrogen. Intensities reported in the excitation profile of $[(d_{21}\text{-}^i Pr_3TACN)_2Cu_2(\mu\text{-}O)_2](PF_6)_2$ were corrected for spectral response of the spectrometer and ν^4 dependence by using the intensity of the acetone solvent peak at 797 cm^{-1} as an internal standard.[48] Depolarization ratios (on-resonance at λ_{ex} = 406.7 nm) and the excitation profile of $[(m\text{-}NO_2PhPyNEt_2)_2Cu_2(\mu\text{-}O)_2](SbF_6)_2$ were determined in acetone solution at −80 °C, and the decomposition kinetics of $[(PhPyNEt_2)_2Cu_2(\mu\text{-}O)_2](SbF_6)_2$ at −70 °C. The low temperature was achieved in a homemade cryostat in which a spinning NMR sample tube was cooled by liquid nitrogen boil off and was maintained to ±1 °C by an in-line resistive heater whose current was controlled by a PID temperature controller. Samples were illuminated in a 135° backscattering geometry. Intensities were calibrated to the large acetone peak as described above. The instrumentation used for scattered light collection, filtering, dispersion, and detection for these experiments has been described elsewhere.[49]

Many of the frequency values in Table 1 are roughly 10 cm^{-1} lower than those originally reported.[2,13,14,16,20,29,32] In the earlier studies, internal solvent bands of THF, acetone, and CH_2Cl_2 were calibrated to literature

(48) Gardiner, D. J. In *Practical Raman Spectroscopy*; Gardiner, D. J., Graves, P. R., Eds.; Springer-Verlag: Heidelberg, 1989; p 11.

(49) Lukat-Rodgers, G. S.; Rodgers, K. R. *Biochemistry* **1997**, *36*, 4178−4187.

values[50] of 680, 806, and 710 cm^{-1}, respectively. However, we subsequently found that these values for liquid samples are *not* accurate for frozen solvents: calibration to emission lines from an Hg lamp shows that these solvent bands shift to 667 cm^{-1} (THF), 797 (acetone), and 702 (CH_2Cl_2) as frozen solids at 77 K. The accuracy of the latter calibration method has been confirmed by means of the tabulated frequencies of solid K_2SO_4 (984 cm^{-1}) and liquid indene,[51] and we believe that spectra calibrated to these new solvent values are trustworthy to ± 1 cm^{-1}. Older spectra have been corrected by retabulating spectra using the correct frozen solvent peak frequencies as a reference, and the frequencies here should be used in place of the earlier values. In new spectra using the CCD system, Raman shifts were referenced internally to the solvent features described above. Spectra in pixel units were converted to frequency units by a quadratic fit of pixels to several peaks in the known spectrum of indene, followed by a spectral shift to give accurate frequencies for the solvent band (this correction was always less than 6 cm^{-1}).

Synthesis and Characterization of [($Me_2N(CH_2)_3NMe_2$)Cu(NCMe)](SbF_6). A solution of tetramethyl-1,3-propanediamine (27 mg, 0.21 mmol) in THF (1 mL) was added to a solution of [Cu(NCMe)$_4$](SbF_6) (96 mg, 0.21 mmol) in 4:1 THF/acetonitrile (2 mL). Addition of diethyl ether (10 mL) and cooling to -30 °C for 1 d gave the product as an analytically pure white powder (82 mg, 83%). ^{1}H NMR (acetone-d_6, 300 MHz): δ 2.77 (m, 4, $Me_2NCH_2CH_2CH_2NMe_2$), 2.56 (s, 12, $Me_2NCH_2CH_2CH_2NMe_2$), 2.40 (s, 3, MeCN), 1.88 (m, 2, $Me_2NCH_2CH_2CH_2NMe_2$) ppm. ^{13}C NMR (acetone-d_6, 300 MHz): δ 117.5 (MeCN), 63.0 ($Me_2NCH_2CH_2CH_2NMe_2$), 48.5 ($Me_2NCH_2CH_2CH_2NMe_2$), 22.9 ($Me_2NCH_2CH_2CH_2NMe_2$), 1.2 (MeCN) ppm. Anal. Calcd for $C_9H_{21}N_3F_6CuSb$: C, 23.03; H, 4.51; N, 8.96. Found: C, 23.06; H, 4.54; N, 8.90.

Computational Methods. Raman spectra were calculated under the harmonic-oscillator rigid-rotator approximation for singlet bis(μ-oxo)dicopper compounds **1**$-$**6** optimized at the density functional level of theory employing the polarized valence double-ζ (pVDZ) basis set of Schafer et al.[52] The gradient-corrected functionals of Becke[53] and of Perdew and Wang[54] (BPW91) were used for exchange and correlation, respectively. All structures were characterized by positive definite Hessian matrixes. Configuration interaction calculations including all single excitations from a restricted Hartree$-$Fock reference[55] were carried out for **2** to establish the nature of the allowed electronic transition observed at long wavelength by UV spectroscopy. Optimization of the triplet state of **2** having the same spatial symmetry as the excited singlet state was also accomplished at the BPW91/pVDZ level. The geometric difference between ground-state (singlet) **2** and triplet **2** was analyzed by using the normal modes of ground-state **2** as a basis, with displacement coefficients determined from multilinear regression.

Appendix

Our analysis of the vibrational frequencies associated with the $[Cu_2O_2]^{2+}$ core was restricted to the four "stretching" normal modes illustrated in Figure 8. Of course, four noncollinear atoms must give rise to a total of six normal modes, not four. For the Cu_2O_2 rhomb, the two modes we did not consider (A_g and B_{1u} symmetry in the D_{2h} point group) have primarily bending character and are expected to have much lower frequencies. To illustrate this point, Table 5 lists all six normal-mode frequencies computed for bare $[Cu_2O_2]^{2+}$ (**7**) at the same level of theory employed for **1**$-$**6** discussed above. Isotope shifts for double ^{18}O substitution are also provided in Table 5. The singlet ground state of **7** has been observed in the gas phase by negative ion photoelectron spectroscopy (NIPES) and has been assigned to have a D_{2h} rhomb structure.[56] The NIPES spectrum reveals a totally symmetric normal mode of 630 $\pm$ 30 cm^{-1}, in fair agreement with computation (these authors note that the normal modes for **7** are very anharmonic).

Table 5. Calculated Freqencies BPW91/pVDZ for the Bare $[Cu_2(\mu\text{-}O)_2]^{2+}$ Core (**7**)

symmetry	$^{16}O_2$ (cm^{-1})	$^{18}O_2$ (cm^{-1})	shift (cm^{-1})
A_g	154.3	153.2	1.1
B_{3u}	203.9	194.6	9.3
B_{1u}	331.2	316.2	15.0
B_{3g}	376.9	359.0	17.9
B_{2u}	403.6	385.3	18.3
A_g	546.7	519.2	27.5

The A_g bending mode is the lowest frequency mode for **7**. The small sensitivity to isotope substitution confirms that this mode involves little Cu$-$O stretching. Additionally, analysis of the normal modes for **1**$-$**6** indicates that this bending mode is heavily mixed with low-frequency ligand motions, so that it does not complicate the Raman analysis presented above.

Finally, we wish to point out that the nature of the two A_g modes in the bis(μ-oxo)dicopper core is quite different from the situation previously described for isomeric (μ-η^2:η^2-peroxo)dicopper cores.[43] In the peroxo compound, the A_g breathing mode is at lower frequency because Cu$-$O bonding is weaker. More importantly, because there is an O$-$O bond, the other A_g mode corresponds not to a rhomb bending motion, but rather to an O$-$O stretching motion that has a much higher frequency ($\sim$750 cm^{-1}). As might be expected, this gives small isotope effects for the breathing mode but very large ones for the O$-$O stretching mode. These points serve to emphasize the difference between the vibrational characteristics of the two isomeric cores; caution should be exercised in comparing one case to the other given their substantially different geometric and electronic structures.

Acknowledgment. The authors thank Dr. Raymond Y. N. Ho for assistance with resonance Raman spectroscopy and recognize the unpublished work on the synthesis, characterization, and oxygen chemistry of [(^{i}Pr$_2$DACO)Cu(NCMe)]$^+$ by Dr. Christopher P. Schaller. Financial support was provided by the NIH (GM47365 to W.B.T., GM33162 to L.Q., and a postdoctoral fellowship to P.L.H.), the NSF (NYI Award to W.B.T., CHE9525819 to C.J.C.), the USDA (96-35305-3628 to K.R.R.), the DOD (f49620-96-1-0359 to K.R.R.), the Herman Frasch Foundation (446-HF97 to K.R.R.), the Alfred P. Sloan Foundation (fellowships to W.B.T. and C.J.C.), and the Camille and Henry Dreyfus Foundation (fellowship to W.B.T.).

Note Added in Proof

While this paper was under review, a complementary work appeared: Henson, M. J.; Mukherjee, P.; Root, D. E.; Stack, T. D. P.; Solomon, E. I. *J. Am. Chem. Soc.* **1999**, *121*, 10332$-$10345.

Supporting Information Available: Tables of resonance Raman spectral data, description of experiments with partially isotopically labeled complexes, the decomposition kinetics of [(PhPyNEt$_2$)$_2$Cu$_2$(μ-O)$_2$](SbF_6)$_2$ as measured by RR spectroscopy, coordinates for the optimized structures of **1**$-$**7**, and a diagram of the core normal modes in **3**$-$**5**. This material is available free of charge via the Internet at http://pubs.acs.org.

JA992003L

(50) *Standard Raman Spectra*; Sadtler Research Laboratories, Inc.: Philadelphia, 1973.
(51) Hamaguchi, H. *Appl. Spectrosc. Rev.* **1988**, *24*, 137$-$174.
(52) Schafer, A.; Horn, H.; Ahlrichs, R. *J. Chem. Phys.* **1992**, *97*, 2571$-$2577.
(53) Becke, A. D. *J. Chem. Phys.* **1986**, *84*, 4524$-$4529.
(54) Perdew, J. P.; Burke, K.; Wang, Y. *Phys. Rev. B* **1996**, *54*, 16533$-$16539.
(55) Foresman, J. B.; Head-Gordon, M.; Pople, J. A.; Frisch, M. J. *J. Phys. Chem.* **1992**, *96*, 135$-$149.
(56) Wang, L.-S.; Wu, H.; Desai, S. R.; Lou, L. *Phys. Rev. B* **1996**, *53*, 8028$-$8031.